



HAL
open science

On the tree gauge in magnetostatics

Francesca Rapetti, Ana Alonso Rodríguez, Eduardo de Los Santos

► **To cite this version:**

Francesca Rapetti, Ana Alonso Rodríguez, Eduardo de Los Santos. On the tree gauge in magnetostatics. Physics, 2022. hal-03426096v1

HAL Id: hal-03426096

<https://hal.science/hal-03426096v1>

Submitted on 12 Nov 2021 (v1), last revised 2 Feb 2022 (v2)

HAL is a multi-disciplinary open access archive for the deposit and dissemination of scientific research documents, whether they are published or not. The documents may come from teaching and research institutions in France or abroad, or from public or private research centers.

L'archive ouverte pluridisciplinaire **HAL**, est destinée au dépôt et à la diffusion de documents scientifiques de niveau recherche, publiés ou non, émanant des établissements d'enseignement et de recherche français ou étrangers, des laboratoires publics ou privés.

On the tree gauge in magnetostatics

Francesca Rapetti ^{1,†}, Ana Alonso Rodríguez ² and Eduardo De Los Santos ²

¹ Affiliation 1; Dept. de Mathématiques, Université Côte d'Azur, Parc Valrose, F-06108 Nice.

² Affiliation 2; Dip. di Matematica, Università degli Studi di Trento, via Sommarive 14, I-38123 Povo, Trento.

* Correspondence: francesca.rapetti@univ-cotedazur.fr (F.R.); ana.alonso@unitn.it (A.A.R.);
ea.delossantosnunez@unitn.it (E.DLS.)

† Corresponding author.

Abstract: We recall the classical tree-cotree technique in magnetostatics. (1) We extend it in the frame of high-order finite elements in general domains. (2) We focus on its connection with the question of the invertibility of the final algebraic system arising from a high-order edge finite element discretization of the magnetostatic problem formulated in terms of the magnetic vector potential. With the same purpose of invertibility, we analyse another classically used condition, the Coulomb gauge. (3) We conclude by underlying that the two gauges can be naturally considered in a high order framework without any restriction on the topology of the domain.

Keywords: magnetic vector potential; high order edge finite elements; tree gauge; Coulomb gauge

1. Introduction

We extend, in an easy way, the classical tree-cotree technique in the frame of high-order finite elements (FEs). We focus on magnetostatics as it represents a significant problem where this technique is usually applied. Particular attention is given to the magnetic vector potential formulation of such a problem. This problem admits infinite solutions hence its discretization by Whitney edge FEs yields to a singular algebraic system.

The techniques that are generally adopted in magnetostatics to eliminate the matrix nullspace are described in two seminal works, one by Albanese and Rubinacci [1] and the other by Cendes and Manges [2]. Albanese and Rubinacci showed that one converts the singular systems, resulting from low-order edge-based discretizations of magnetostatic problems, into nonsingular ones by setting to zero the vector potential circulations on a spanning tree edges of the FE mesh graph. Manges and Cendes underlined the relation between the tree-cotree approach proposed by Albanese and Rubinacci and the imposition of the Coulomb gauge in a discrete manner.

With classical edge FEs, the degrees of freedom (dofs) are the circulations of the approximated vector field along the edges of the FE mesh [3]. Hence, tree-cotree techniques are perfectly adapted to this type of discretizations since there is a one-to-one correspondence between edges, listed in the tree or cotree sets, and dofs.

In a high order FE discretization of the same problem, the dofs introduced in [4], the so-called weights, have again a physical signification. For edge discretizations, they have the meaning of circulations on suitable edges of a fictitious refinement of the FE mesh. This fact allows to rely in a very natural way on tree-cotree techniques. These new dofs were born from using the same geometrical approach, proposed by Whitney [5] to construct low order polynomial representations of differential forms, on a finer simplicial complex of the computational domain mesh. These weights do coincide with Whitney edge FE dofs in the low-order case.

In these pages, by relying on linear algebra, we analyse the fundamental work accomplished in the 90s on tree-cotree techniques and show that it is still of actuality in the

Citation: Rapetti, F.; Alonso Rodríguez, A.; De Los Santos, E. On the tree gauge in magnetostatics. *J* **2021**, *1*, 1–11. <https://doi.org/>

Received:

Accepted:

Published:

Publisher's Note: MDPI stays neutral with regard to jurisdictional claims in published maps and institutional affiliations.

Copyright: © 2021 by the authors. Submitted to *J* for possible open access publication under the terms and conditions of the Creative Commons Attribution (CC BY) license (<https://creativecommons.org/licenses/by/4.0/>).

39 high order case when fields are reconstructed in the discrete space by using their weights.
40

We thus start by considering an open bounded connected polyhedral domain $\Omega \subset \mathbb{R}^3$ with boundary $\partial\Omega$. We indicate by $(\partial\Omega)_j$, for $j = 0, \dots, p$, the connected components of $\partial\Omega$ (in particular, $(\partial\Omega)_0$ is the external one). We denote by g the number of independent non-bounding cycles in Ω . Note that $b_1(\Omega) = g$ and $b_2(\Omega) = p$ are, respectively, the first and the second Betti numbers of Ω . For a domain $\Omega \subset \mathbb{R}^3$, the 0th Betti number $b_0(\Omega)$ is equal to m , the number of connected components of Ω . If Ω is connected, as assumed in these pages, $m = 1$. The third Betti number $b_3(\Omega) = 0$ in the present case. Betti numbers describe the topology of Ω and provide a way of computing its Euler-Poincaré characteristic as the number $\chi(\Omega) = b_0 - b_1 + b_2 - b_3$. We introduce the space

$$\mathcal{H}_\mu(m; \Omega) = \{\mathbf{w} \in (L^2(\Omega))^3, \mathbf{curl} \mathbf{w} = \mathbf{0}, \operatorname{div}(\mu \mathbf{w}) = 0, \mu \mathbf{w} \cdot \mathbf{n}_{\partial\Omega} = 0 \text{ on } \partial\Omega\}.$$

Note that $\dim(\mathcal{H}_\mu(m; \Omega)) = g (= b_1(\Omega))$. The magnetostatic problem in its most basic form reads: find the magnetic induction field \mathbf{B} due to prescribed compatible currents \mathbf{J} and defined by the field equations and conditions

$$\begin{aligned} \mathbf{curl}(\mu^{-1}\mathbf{B}) &= \mathbf{J}, & \text{in } \Omega, \\ \operatorname{div} \mathbf{B} &= 0, & \text{in } \Omega, \\ \mathbf{B} \cdot \mathbf{n}_{|\partial\Omega} &= 0, & \text{on } \partial\Omega, \\ \int_{\Omega} \mu^{-1}\mathbf{B} \cdot \mathbf{w} &= 0, & \forall \mathbf{w} \in \mathcal{H}_\mu(m; \Omega). \end{aligned} \tag{1}$$

41 Here above, $\mathbf{n}_{|\partial\Omega}$ is the outward going unit normal to $\partial\Omega$ and μ the magnetic perme-
42 ability of the material contained in Ω . It is assumed that $\mu \in L^\infty(\Omega)$ is symmetric and
43 positive definite, bounded from below, namely, $\mu \geq \mu_0 > 0$ for a real number μ_0 (that co-
44 incides with the magnetic permeability of the air). The last condition of L^2 -orthogonality
45 to the space $\mathcal{H}_\mu(m; \Omega)$ is of key importance to guarantee the solution uniqueness. Indeed,
46 when $\mathbf{J} = \mathbf{0}$, the first three equations in (1) give $\mu^{-1}\mathbf{B} \in \mathcal{H}_\mu(m; \Omega)$ that, together with
47 the last condition, yields $\mu^{-1}\mathbf{B} = \mathbf{0}$, that means $\mathbf{B} = \mathbf{0}$, due to the properties of μ (see
48 more details in [6]). For compatible currents, we mean \mathbf{J} such that $\operatorname{div} \mathbf{J} = 0$ in Ω and
49 $\int_{(\partial\Omega)_j} \mathbf{J} \cdot \mathbf{n}_{|\partial\Omega} = 0$, for any j th (out of $p+1$) connected component $(\partial\Omega)_j$ of $\partial\Omega$.

50 The paper layout is as follows. In section 2, we reformulate problem (1) in terms of
51 the magnetic vector potential and its weak formulation. We thus define the high-order
52 FE approximation space and write the discrete problem together with its matrix form
53 in section 3. In section 4 we present the tree-cotree approach and the analysis of the
54 linear system to solve in the block form dictated by the tree. Section 5 is dedicated to
55 the Coulomb gauge. We briefly discuss in Section 6 about the other formulation of the
56 magnetostatic problem and on its connection with the tree-cotree approach. We conclude
57 in Section 7 by analysing differences and similarities between the presented gauges.

58 2. The magnetic vector potential problem

A way to exactly satisfy the solenoidality condition $\operatorname{div} \mathbf{B} = 0$ on the magnetic induction field \mathbf{B} is to represent \mathbf{B} in terms of a vector potential, namely a vector \mathbf{A} such that $\mathbf{B} = \mathbf{curl} \mathbf{A}$. This magnetic potential \mathbf{A} is not uniquely defined as the vector $\tilde{\mathbf{A}} = \mathbf{A} + \mathbf{grad} V$, for V a scalar function, still verifies $\mathbf{B} = \mathbf{curl} \tilde{\mathbf{A}}$. A classical way to ensure the uniqueness of \mathbf{A} is to prescribe a gauge condition on \mathbf{A} , *e.g.*, the Coulomb gauge $\operatorname{div}(\mu \mathbf{A}) = 0$. We introduce the space

$$\mathcal{H}_\mu(e; \Omega) = \{\mathbf{w} \in (L^2(\Omega))^3, \mathbf{curl} \mathbf{w} = \mathbf{0}, \operatorname{div}(\mu \mathbf{w}) = 0, \mathbf{w} \times \mathbf{n}_{\partial\Omega} = \mathbf{0} \text{ on } \partial\Omega\}.$$

Note that $\dim(\mathcal{H}_\mu(e; \Omega)) = p (= b_2(\Omega))$. The magnetostatic problem (1) thus reads: given a compatible \mathbf{J} , find a vector \mathbf{A} satisfying the field equations

$$\begin{aligned} \mathbf{curl} \mu^{-1} \mathbf{curl} \mathbf{A} &= \mathbf{J} && \text{in } \Omega, \\ \operatorname{div}(\mu \mathbf{A}) &= 0 && \text{in } \Omega, \\ \mathbf{A} \times \mathbf{n}|_{\partial\Omega} &= \mathbf{0} && \text{on } \partial\Omega, \\ \int_{(\partial\Omega)_j} \mu \mathbf{A} \cdot \mathbf{n}_{\partial\Omega} &= 0 && \forall j = 0, \dots, p. \end{aligned} \quad (2)$$

59 Note that from the condition $\mathbf{A} \times \mathbf{n}|_{\partial\Omega} = \mathbf{0}$ follows $\mathbf{curl} \mathbf{A} \cdot \mathbf{n}|_{\partial\Omega} = 0$ hence $\mathbf{B} \cdot \mathbf{n}|_{\partial\Omega} = 0$. It
60 is possible to show (see again [6]) that $\mathbf{grad}(z_j) \in \mathcal{H}_\mu(e; \Omega)$ for each function $z_j \in H^1(\Omega)$
61 that is solution of $\operatorname{div}(\mu \mathbf{grad} z_j) = 0$ in Ω , with boundary conditions $(z_j)|_{(\partial\Omega)_i} = \delta_{ij}$,
62 for $i, j = 0, \dots, p$ (here δ_{ij} is the Kronecker symbol). If $\mathbf{J} = \mathbf{0}$, we have $\mathbf{curl} \mathbf{A} = \mathbf{0}$. If
63 $\operatorname{div}(\mu \mathbf{A}) = 0$ and $\int_{\Omega} \mu \mathbf{A} \cdot \mathbf{grad} z_j = 0$ then $\int_{(\partial\Omega)_j} \mu \mathbf{A} \cdot \mathbf{n}_{\partial\Omega} = 0$, for each $j = 0, \dots, p$.

In view of using FEs, we need to rewrite problem (2) in weak form. We multiply the first equation of (2) by a test function $\mathbf{v} \in H_0(\mathbf{curl}; \Omega)$ where $H_0(\mathbf{curl}; \Omega) = \{\mathbf{u} \in (L^2(\Omega))^3, \mathbf{curl} \mathbf{u} \in (L^2(\Omega))^3, \mathbf{u} \times \mathbf{n}|_{\partial\Omega} = \mathbf{0}\}$. We then integrate by parts over Ω to obtain

$$\int_{\Omega} \mu^{-1} \mathbf{curl} \mathbf{A} \cdot \mathbf{curl} \mathbf{v} = \int_{\Omega} \mathbf{J} \cdot \mathbf{v}, \quad \forall \mathbf{v} \in H_0(\mathbf{curl}; \Omega). \quad (3)$$

Condition $\operatorname{div}(\mu \mathbf{A}) = 0$ yields the following characterisation for \mathbf{A} in Ω :

$$\int_{\Omega} \operatorname{div}(\mu \mathbf{A}) \varphi = 0, \quad \forall \varphi \in C_c^\infty(\Omega), \quad (4)$$

being $C_c^\infty(\Omega)$ the space of smooth functions with compact support in Ω . By integration by parts and applying a density argument, we can write

$$\int_{\Omega} \mu \mathbf{A} \cdot \mathbf{grad} \varphi = 0, \quad \forall \varphi \in H_0^1(\Omega), \quad (5)$$

and (5) yields $\operatorname{div}(\mu \mathbf{A}) = 0$ in Ω (in the sense of distributions). When $p > 0$, the second and fourth equations in problem (2) can be imposed by using (5) with $\varphi \in H_*^1(\Omega) = \{\varphi \in H^1(\Omega), \varphi|_{(\partial\Omega)_j} = c_j, \forall j = 0, \dots, p\}$ where $\mathbf{c} \in \mathbb{R}^{p+1}$ is a constant vector. In fact, taking $z_i \in H_*^1(\Omega)$, with $c_j = \delta_{ij}$ for all $i, j = 0, \dots, p$, we have

$$0 = \int_{\Omega} \mu \mathbf{A} \cdot \mathbf{grad} z_i = - \int_{\Omega} \operatorname{div}(\mu \mathbf{A}) z_i + \int_{\partial\Omega} \mu \mathbf{A} \cdot \mathbf{n}_{\partial\Omega} z_i = \int_{(\partial\Omega)_i} \mu \mathbf{A} \cdot \mathbf{n}_{\partial\Omega}.$$

So, we look for $\mathbf{A} \in H_0(\mathbf{curl}; \Omega)$ such that (3) holds together with the condition

$$\int_{\Omega} \mu \mathbf{A} \cdot \mathbf{grad} \varphi = 0, \quad \forall \varphi \in H_*^1(\Omega). \quad (6)$$

64 3. The discrete problem and its matrix form

Let $\tau_h = (V, E, F, T)$ be a simplicial triangulation over Ω and $\Omega_h = \cup_{t \in T} t$. Even if τ_h is a simplicial triangulation of Ω , the topological properties computed on Ω_h are the same as those of Ω . For Ω connected, with g loops and p cavities, the Euler-Poincaré characteristics $\chi(\Omega)$ and $\chi(\Omega_h)$ are equal and we have

$$(\chi(\Omega) = b_0 - b_1 + b_2 - b_3 =) \quad 1 - g + p = n_V - n_E + n_F - n_T \quad (= \chi(\Omega_h))$$

65 where n_V, n_E, n_F, n_T are, respectively, the cardinalities of the sets of vertices V , edges E ,
66 faces F and tetrahedra T of the mesh τ_h . Given a simplicial mesh τ_h over $\bar{\Omega}$, we denote by
67 $W_{r+1}^k = \mathcal{P}_{r+1}^- \Lambda^k(\tau_h)$ the set of Whitney differential k -forms of polynomial degree $r + 1$,
68 where $k \in \{0, 1, 2, 3\}$ is the order of the form (see [7] for more details on the properties of
69 these spaces). It is a compact notation to indicate space of polynomial functions which
70 are well-known in finite elements. Indeed, for $k = 0$, we have $W_{r+1}^0 = L_{r+1}$, the space of

71 continuous, piecewise polynomials of degree $r + 1$; for $k = 1$, we obtain $W_{r+1}^1 = N_{r+1}$
 72 the first family of Nédélec edge element functions of degree $r + 1$; for $k = 2$, we get
 73 $W_{r+1}^2 = RT_{r+1}$ the space of Raviart-Thomas functions of degree $r + 1$; for $k = 3$, we
 74 find $W_{r+1}^3 = P_r$ discontinuous piecewise polynomials of degree r . The spaces W_{r+1}^k
 75 are connected in a complex by linear operators which can be represented by suitable
 76 matrices, namely G ($k = 0$), R ($k = 1$), D ($k = 2$) respectively, once a set of unisolvent
 77 dofs and consequently a basis in each space W_{r+1}^k have been fixed. Note that the entries
 78 of these matrices are $0, \pm 1$, only for few bases of these spaces W_{r+1}^k associated with dofs
 79 chosen as, for example, the *weights* of a physical field, intended as a differential k -form,
 80 on chains of k -simplices of the high-order FE mesh.

81 For $r = 0$, the dimension of the space W_1^k coincides with the number of k -simplices in
 82 the mesh, indeed $\dim L_1 = n_V$, $\dim N_1 = n_E$, $\dim RT_1 = n_F$ and $\dim P_0 = n_T$. Moreover,
 83 the matrices G, R, D are, resp., the edge-to-node, face-to-edge and tetrahedron-to-face
 84 connectivity matrices taking also into account respective orientations. Dofs for fields in
 85 W_1^k are, respectively, their values at the mesh nodes ($k = 0$), their circulations along the
 86 edges ($k = 1$), their fluxes across the mesh faces ($k = 2$) and their densities at the mesh
 87 tetrahedra ($k = 3$).

88 For $r > 0$, as explained in [4], by connecting the nodes of the principal lattice of
 89 degree $r + 1$ in a n -simplex $t \in T$, we obtain a number of *small n -simplices* that are
 90 $1/(r + 1)$ -homothetic to t . The *small k -simplices*, $0 \leq k < n$, are all the k -simplices
 91 that compose the boundary of the small n -simplices. Any small k -simplex is denoted
 92 by a couple $\{\alpha, s\}$, with s a k -simplex of τ_h and α is a multi-integer $(\alpha_0, \dots, \alpha_n)$ with
 93 $\sum_{i=0}^n \alpha_i = r$, $\alpha_i \in \mathbb{Z}$ and $\alpha_i \geq 0$. The term *active* is to indicate all couples $\{\alpha, s\}$ such that
 94 the function $\lambda^\alpha \mathbf{w}^s$ belongs to a basis of W_{r+1}^k , where $\lambda^\alpha = \lambda_0^{\alpha_0} \lambda_1^{\alpha_1} \dots \lambda_n^{\alpha_n}$ and $\mathbf{w}^s \in W_1^k$.
 95 Indeed, by considering all possible multi-indices α in the couples $\{\alpha, s\}$, one generates
 96 more functions $\lambda^\alpha \mathbf{w}^s$ than necessary. The dimension of the space W_{r+1}^k coincides with the
 97 number of *active small k -simplices* in the mesh. The small k -simplices were born to define
 98 a set of unisolvent dofs, the weights $\int_{\{\alpha, s\}} u$, for functions $u \in W_{r+1}^k(t)$ when $r > 0$, that,
 99 differently from the classical moments, maintain a physical interpretation. About the
 100 weights, their definition was first given in [4] and unisolvence, despite redundancies,
 101 proved in [8]. For the unisolvence of a minimal (*i.e.*, without redundancies) set of such
 102 weights, we refer to [9].

103 This work relies on the spaces W_{r+1}^0 and W_{r+1}^1 . In particular, the meaning of the
 104 matrix G is the same as for the case $r = 0$ provided that we work with the active small
 105 k -simplices instead of the k -simplices of the mesh τ_h , with $k = 0, 1$. The weights for high
 106 order Lagrangian finite elements W_{r+1}^0 are the values of the function at the points of the
 107 corresponding principal lattice of each tetrahedron of the mesh, and the weights for high
 108 order Nédélec finite elements W_{r+1}^1 are the line integrals of the vector field along the
 109 active small edges connecting adjacent points of the principal lattice. The geometrical
 110 realization of the graph \mathcal{G} associated with the gradient operator, is straightforward (see
 111 an example in triangles, for $r + 1 = 4$, in Figure 1, the picture in second position from
 112 the left). A spanning tree \mathcal{T}^G is a maximal subgraph of \mathcal{G} (maximal because it visits
 113 all vertices of \mathcal{G}) without closing circuits (this means that it is a tree). The remaining
 114 subgraph $\mathcal{G} \setminus \mathcal{T}^G$ is called the cotree. An example of spanning tree and associated cotree
 115 in triangles, for $r + 1 = 4$, is given in Figure 1, the last two pictures on the right. In a
 116 mesh, a similar construction is used to enrich a spanning tree of the vertices-edges graph
 117 of the mesh.

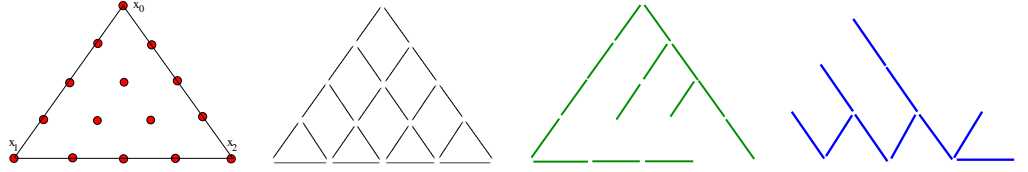


Figure 1. For $r + 1 = 4$, in a mesh triangle $t = [x_0, x_1, x_2]$, from left to right, are drawn, respectively, the small nodes of the principal lattice, the active small edges of the graph \mathcal{G} associated with the small-edge-to-small-node incidence matrix G , a spanning tree in \mathcal{G} and its cotree.

118 The meaning of G as edge-to-node connectivity matrix is thus the same as that for
 119 the case $r = 0$, provided that we work with the active small edges of the high-order FE
 120 mesh in Ω_h instead of the edges of τ_h . From now on, d_L (resp. d_N) denotes the cardinality
 121 of the set of nodes or small nodes (resp. edges or active small edges) whatever $r \geq 0$ is,
 122 and the terms *active* and *small* for k -simplices are taken for granted. We now make for
 123 the discrete problem.

Let $\{\mathbf{w}_j\}_{j=1, \dots, d_N}$ be the (dual) basis for $W^1 = W_{r+1}^1 \cap H_0(\mathbf{curl}; \Omega)$ (for simplicity, we keep on denoting by d_N the dimension of W^1 and d_L that of $W^0 = W_{r+1}^0 \cap H_0^1(\Omega)$) with respect to the weights over the active small edges as dofs, i.e., $\int_{\{\boldsymbol{\alpha}, e\}_\ell} \mathbf{w}_j = \delta_{j,\ell}$ for all $\ell = 1, \dots, d_N$. The discretization of the variational formulation (3) is stated as: find $\mathbf{A}_h \in W^1$, such that

$$\int_{\Omega} \mu^{-1} \mathbf{curl} \mathbf{A}_h \cdot \mathbf{curl} \mathbf{v}_h = \int_{\Omega} \mathbf{J} \cdot \mathbf{v}_h, \quad \forall \mathbf{v}_h \in W^1. \quad (7)$$

If we write $\mathbf{A}_h = \sum_{j=1}^{d_N} a_j \mathbf{w}_j$ and select $\mathbf{v}_h = \mathbf{w}_i$ for all $i \in \{1, \dots, d_N\}$, the discrete variational problem results in the linear algebraic system

$$\mathbf{S} \mathbf{a} = \mathbf{b}, \quad (8)$$

where

$$S_{i,j} = \int_{\Omega} \mu^{-1} \mathbf{curl} \mathbf{w}_j \cdot \mathbf{curl} \mathbf{w}_i, \quad b_i = \int_{\Omega} \mathbf{J} \cdot \mathbf{w}_i, \quad a_j = \int_{\{\boldsymbol{\alpha}, e\}_j} \mathbf{A} \cdot \boldsymbol{\tau}_j, \quad (9)$$

and $\{\boldsymbol{\alpha}, e\}_j$ is the j th active small edge with unit tangent vector $\boldsymbol{\tau}_j$. The discrete form of condition (6) reads:

$$\int_{\Omega} \mu \mathbf{A}_h \cdot \mathbf{grad} \varphi_h = 0, \quad \forall \varphi_h \in W_*^0, \quad (10)$$

124 with $W_*^0 = W_{r+1}^0 \cap H_*^1(\Omega)$. Condition (10) says that \mathbf{A}_h is orthogonal to $\mathbf{grad}(W_*^0)$. With
 125 the help of the tree-cotree technique we will see, in a general domain, the conditions
 126 for the invertibility of system (8) imposed by the tree gauge and those by the discrete
 127 Coulomb gauge (10).

128 4. The tree-cotree decomposition to analyse the system $\mathbf{S} \mathbf{a} = \mathbf{b}$

To accomplish the first step, we characterize the nullspace of S , namely the set of vectors \mathbf{a} such that $\mathbf{S} \mathbf{a} = \mathbf{0}$. Correspondingly, we have

$$\int_{\Omega} \mu^{-1} \mathbf{curl} \mathbf{A}_h \cdot \mathbf{curl} \mathbf{v}_h = 0, \quad \forall \mathbf{v}_h \in W^1. \quad (11)$$

Selecting $\mathbf{v}_h = \mathbf{A}_h$, we write (11) as

$$0 = \int_{\Omega} (\mathbf{curl} \mathbf{A}_h)^\top \mu^{-1} \mathbf{curl} \mathbf{A}_h \geq C \|\mathbf{curl} \mathbf{A}_h\|_{L^2(\Omega)}^2, \quad (12)$$

129 where the constant $C > 0$ depends on μ . For this reason, from (12) we deduce that
 130 $\mathbf{curl} \mathbf{A}_h = \mathbf{0}$. Then $\mathbf{S} \mathbf{a} = \mathbf{0} \Rightarrow \mathbf{curl} \mathbf{A}_h = \mathbf{0} \Rightarrow \mathbf{R} \mathbf{a} = \mathbf{0}$, where \mathbf{R} is the active small-

131 face-to-small-edge connectivity matrix. Since $\mathbf{S}\mathbf{a} = \mathbf{0}$ if and only if $\mathbf{R}\mathbf{a} = \mathbf{0}$, then S
 132 and R share the same nullspace $\text{Ker}(S) = \text{Ker}(R)$, therefore, they are row equivalent
 133 $\text{Row}(S) \oplus \text{Ker}(S) = \mathbb{R}^{d_N} = \text{Row}(R) \oplus \text{Ker}(R) \Rightarrow \text{Row}(S) = \text{Row}(R)$.

Identifying the free variables corresponding to $R \in \mathbb{R}^{d_{RT} \times d_N}$ (with more columns than rows, namely $d_N > d_{RT}$) is possible by a tree-cotree decomposition (e.g., as it was done in the last row of [10, eqn. 3]). Namely, we set to zero all the variables associated with a spanning tree \mathcal{T}^G of a suitable graph \mathcal{G}^* derived from the graph \mathcal{G} of the gradient operator G . The construction of the graph \mathcal{G}^* from \mathcal{G} is done as follows. In the graph \mathcal{G} , since $\mathbf{A} \times \mathbf{n}_{|\partial\Omega} = \mathbf{0}$, for each $j = 0, \dots, p$, we eliminate all the active small edges $\{\alpha, e\}$ lying on the connected component $(\partial\Omega)_j$. To do this, we collapse all their extremities into a unique node, say \mathbf{x}_j^* . Accordingly, an active small edge, say $\{\alpha, e\} = [\mathbf{x}_0, \mathbf{x}_1]$, with one extremity at a node $\mathbf{x}_0 \notin \partial\Omega$ and the other extremity at a node $\mathbf{x}_1 \in (\partial\Omega)_j$, is deformed (\rightsquigarrow) into an edge, still denoted by $\{\alpha, e\}$, with extremity \mathbf{x}_0 and \mathbf{x}_j^* , that is $[\mathbf{x}_0, \mathbf{x}_1] \rightsquigarrow [\mathbf{x}_0, \mathbf{x}_j^*]$. We thus get a modified graph $\mathcal{G}^* = (\mathcal{N}^*, \mathcal{E}^*)$ with vertices, the set

$$\mathcal{N}^* = \{\mathbf{x}_0 \in \mathcal{G}, \mathbf{x}_0 \notin \partial\Omega\} \cup_{j=0, \dots, p} \{\mathbf{x}_j^*\},$$

and arcs, the set defined as

$$\mathcal{E}^* = \{[\mathbf{x}_0, \mathbf{x}_1], \text{ both } \mathbf{x}_0, \mathbf{x}_1 \notin \partial\Omega\} \cup_{j=0, \dots, p} \{[\mathbf{x}_0, \mathbf{x}_1] \rightsquigarrow [\mathbf{x}_0, \mathbf{x}_j^*], \mathbf{x}_0 \notin \partial\Omega, \mathbf{x}_1 \in (\partial\Omega)_j\},$$

134 that is the set of small edges $\{\alpha, e\}$ edges of \mathcal{G} with both extremities not on $\partial\Omega$ together
 135 with the set of the deformed ones, namely those small edges of \mathcal{G} with an extremity on
 136 $\partial\Omega$ that has collapsed into one of the nodes \mathbf{x}_j^* .

Taking advantage of the row equivalence between R and S (following the ideas of Manges and Cendes [2]), we decompose S into blocks, corresponding with a partition of the active small edges in two sets, by relying on a spanning tree of the graph of the gradient operator G of the high-order FE mesh. Dofs supported by small edges out of the tree (thus on the so-called cotree), are numbered first, and dofs corresponding with small edges on the tree are numbered second. The subscript *ct* (resp., *t*) indicates the block of indices associated with small edges in the complement of the spanning tree (resp., in the spanning tree), namely, $\mathbf{a} = [\mathbf{a}_{ct}, \mathbf{a}_t]^\top$. According to this decomposition, the system (8) reads

$$\begin{bmatrix} S_{ct,ct} & S_{ct,t} \\ S_{t,ct} & S_{t,t} \end{bmatrix} \begin{bmatrix} \mathbf{a}_{ct} \\ \mathbf{a}_t \end{bmatrix} = \begin{bmatrix} \mathbf{b}_{ct} \\ \mathbf{b}_t \end{bmatrix}. \quad (13)$$

137 Note that S is a singular matrix and this mimics the singularity of the continuous
 138 problem (2). The singularity of S raises two issues. First, compatibility, namely, which
 139 are the requirements on \mathbf{b} so that \mathbf{b} is in the range of S ? Secondly, uniqueness, namely is
 140 there a way to ensure uniqueness for the solution of (8), under compatibility condition?

141 4.1. Characterising the block of maximal rank in the system matrix

142 The tree-cotree technique provides a way to define the set of indices *ct* (corresponding
 143 with dofs associated with the cotree) such that $S_{ct,ct}$ is maximal rank. Indeed, we
 144 have the following result.

145 **Theorem 1.** *The square block $S_{ct,ct}$ is invertible.*

Proof of Theorem 1. Let us denote by q the size of $S_{ct,ct}$ and let us consider a vector $\mathbf{z} \in \mathbb{R}^q$ such that $\mathbf{z} \in \text{ker}(S_{ct,ct})$. Hence, $S_{ct,ct} \mathbf{z} = \mathbf{0}$ and $\mathbf{z}^\top S_{ct,ct} \mathbf{z} = 0$, too. We have

$$0 = \mathbf{z}^\top S_{ct,ct} \mathbf{z} = \int_{\Omega} \mu^{-1} \mathbf{curl} \mathbf{Z}_h \cdot \mathbf{curl} \mathbf{Z}_h,$$

where $\mathbf{Z}_h = \sum_{j \in ct} \mathbf{z}_j \mathbf{w}_j$ is an element of W^1 . Due to the requirement on μ , this gives $\mathbf{curl} \mathbf{Z}_h = \mathbf{0}$. As a consequence, $\mathbf{Z}_h = \mathbf{grad} \psi_h$ for a scalar field $\psi_h \in W_*^0$. Let us check that this yields $\mathbf{Z}_h = \mathbf{0}$. Indeed, each small edge $\{\alpha, e\}_j$ of the cotree ($j \in ct$) closes, together with other arcs $\{\beta, e\}_k$ that all belong to the tree ($k \in t$), a circuit γ in the mesh graph. Being \mathbf{Z}_h equal to the gradient of a scalar function, its circulation on circuits is zero. Note \mathbf{Z}_h has the form $\mathbf{Z}_h = \sum_{j \in ct} \mathbf{z}_j \mathbf{w}_j + \sum_{k \in t} \mathbf{0} \mathbf{w}_k$. We thus have

$$\oint_{\gamma} \mathbf{Z}_h \cdot \boldsymbol{\tau}_{\gamma} = 0 = \int_{\{\alpha, e\}_j} \mathbf{Z}_h \cdot \boldsymbol{\tau}_{\gamma} + \int_{\gamma \setminus \{\alpha, e\}_j} \mathbf{Z}_h \cdot \boldsymbol{\tau}_{\gamma} = \mathbf{z}_j + 0.$$

146 So, $\mathbf{z}_j = \mathbf{0}$ for each edge $\{\alpha, e\}_j$ in the cotree, that yields $\mathbf{z} = \mathbf{0}$ and the invertibility of
147 $S_{ct,ct}$. \square

148 We wish to underline a property that will be widely applied in the following:

149

150 **Property:** If $S_{ct,ct}$ has maximal rank q , then $S_{\Gamma} = S_{t,t} - S_{t,ct} S_{ct,ct}^{-1} S_{ct,t} = 0$.

Proof of the Property. If the first q lines (block ct) in (13) define the rank of S , the remaining $(d_N - q)$ lines (block t) are linear combination of the first q ones. This means that it exists a matrix $C \in \mathbb{R}^{(d_N - q) \times q}$ such that

$$\begin{bmatrix} S_{t,ct} & S_{t,t} \end{bmatrix} = C \begin{bmatrix} S_{ct,ct} & S_{ct,t} \end{bmatrix}$$

151 Therefore, $S_{\Gamma} = C S_{ct,t} - C S_{ct,ct} S_{ct,ct}^{-1} S_{ct,t} = C S_{ct,t} - C S_{ct,t} = 0$. \square

152 For a matrix M , the expression $M_{\Gamma} = [M_{t,t} - M_{t,ct} M_{ct,ct}^{-1} M_{ct,t}]$ is well known in
153 the frame of domain decomposition (DD) methods, indeed it coincides with the so-called
154 Schur complement associated with M for the partition of indices into the sets ct and t .
155 In the context of DD methods, it is not used to put in evidence the maximal rank block
156 of M , since M in the DD context is an invertible matrix, but rather to solve $M\mathbf{a} = \mathbf{b}$
157 by going through the inversion of a finite number of better conditioned smaller linear
158 systems (the interested reader can find more details in [11]).

159 4.2. Requirements on the system right-hand-side for the existence of a solution

160 We now focus on the compatibility condition for the right-hand-side of (13). It is
161 an algebraic constraint for a vector \mathbf{b} to be the right-hand-side of a linear system with
162 matrix S , thus stating when $\mathbf{b} \in \text{Im}(S) = \{S\mathbf{v}, \mathbf{v} \in \mathbb{R}^{d_N}\}$.

163 **Theorem 2.** $\mathbf{b} \in \text{Im}(S)$ if and only if $\mathbf{b}_t = S_{t,ct} S_{ct,ct}^{-1} \mathbf{b}_{ct}$.

Proof of Theorem 2. The fact that $\mathbf{b} \in \text{Im}(S)$ implies \mathbf{b} is in the columns space of S , so
 $\mathbf{b} = S\mathbf{z}$ for some $\mathbf{z} \in \mathbb{R}^{d_N}$. Written in partitioned matrix form

$$\begin{bmatrix} \mathbf{b}_{ct} \\ \mathbf{b}_t \end{bmatrix} = \begin{bmatrix} S_{ct,ct} & S_{ct,t} \\ S_{t,ct} & S_{t,t} \end{bmatrix} \begin{bmatrix} \mathbf{z}_{ct} \\ \mathbf{z}_t \end{bmatrix} \quad (14)$$

This yields the equations

$$S_{ct,ct}^{-1} \mathbf{b}_{ct} = \mathbf{z}_{ct} + S_{ct,ct}^{-1} S_{ct,t} \mathbf{z}_t \quad \text{and} \quad \mathbf{b}_t = S_{t,ct} \mathbf{z}_{ct} + S_{t,t} \mathbf{z}_t. \quad (15)$$

Thanks to the fact that $\text{rank}(S) = \text{rank}(S_{ct,ct})$, we know that $[S_{t,t} - S_{t,ct} S_{ct,ct}^{-1} S_{ct,t}] = 0$. By
eliminating \mathbf{z}_{ct} in (15) and considering $S_{t,t} = S_{t,ct} S_{ct,ct}^{-1} S_{ct,t}$ in (15), we have the following
relation between the blocks of \mathbf{b} :

$$\mathbf{b}_t = S_{t,ct} S_{ct,ct}^{-1} \mathbf{b}_{ct}, \quad (16)$$

164 that is what we wished to prove. \square

165 Condition (16) has to be satisfied by \mathbf{b} to be in the range of S , prior to solving (8).

166 4.3. Characterising the nullspace of the system matrix

167 Under a compatibility condition on the right-hand side \mathbf{b} addressed in the previous
168 section, the nullspace of S is responsible for the lack of uniqueness of the solution \mathbf{a} . We
169 thus characterise the nullspace of S , i.e., $\ker(S) = \{\mathbf{v} \in \mathbb{R}^{d_N}, S\mathbf{v} = \mathbf{0}\}$.

170 **Theorem 3.** $\mathbf{a} \in \ker(S)$ if and only if $\mathbf{a}_{ct} = -S_{ct,ct}^{-1} S_{ct,t} \mathbf{a}_t$.

Proof of Theorem 3. Let $\mathbf{a} \in \ker(S)$. Under the form (13), the first block of lines in the system $S\mathbf{a} = \mathbf{0}$ reads $S_{ct,ct} \mathbf{a}_{ct} + S_{ct,t} \mathbf{a}_t = \mathbf{0}$. Being $S_{ct,ct}$ invertible, we get $\mathbf{a}_{ct} = -S_{ct,ct}^{-1} S_{ct,t} \mathbf{a}_t$. The other way around, if $\mathbf{a}_{ct} = -S_{ct,ct}^{-1} S_{ct,t} \mathbf{a}_t$, then the vector $\mathbf{b} = S\mathbf{a}$ reads

$$\begin{bmatrix} \mathbf{b}_{ct} \\ \mathbf{b}_t \end{bmatrix} = \begin{bmatrix} S_{ct,ct} & S_{ct,t} \\ S_{t,ct} & S_{t,t} \end{bmatrix} \begin{bmatrix} -S_{ct,ct}^{-1} S_{ct,t} \mathbf{a}_t \\ \mathbf{a}_t \end{bmatrix} = \begin{bmatrix} \mathbf{0} \\ (S_{t,t} - S_{t,ct} S_{ct,ct}^{-1} S_{ct,t}) \mathbf{a}_t \end{bmatrix}.$$

171 Hence $\mathbf{b}_{ct} = \mathbf{0}$ and $\mathbf{b}_t = S_{\Gamma} \mathbf{a}_t$ with $S_{\Gamma} = (S_{t,t} - S_{t,ct} S_{ct,ct}^{-1} S_{ct,t})$. We have that $\mathbf{b}_t = \mathbf{0}$,
172 too, because $S_{\Gamma} = 0$ since $\text{rank}(S_{ct,ct}) = \text{rank}(S)$. So $\mathbf{a} \in \ker(S)$. \square

If \mathbf{b} verifies (16) then $\mathbf{b} \in (\ker(S))^{\perp}$. Indeed, by a simple calculation, we have $\mathbf{b} \cdot \mathbf{w} = 0$ for all $\mathbf{w} \in \ker(S)$. In fact, $\mathbf{b} \cdot \mathbf{w} = \mathbf{b}_{ct} \cdot \mathbf{w}_{ct} + \mathbf{b}_t \cdot \mathbf{w}_t$. By relying on (16) and Theorem 3 for \mathbf{w} , we have

$$\mathbf{b}_{ct} \cdot \mathbf{w}_{ct} + \mathbf{b}_t \cdot \mathbf{w}_t = -\mathbf{b}_{ct}^{\top} S_{ct,ct}^{-1} S_{ct,t} \mathbf{w}_t + (S_{t,ct} S_{ct,ct}^{-1} \mathbf{b}_{ct})^{\top} \mathbf{w}_t = 0$$

173 since $(S_{ct,ct}^{-1})^{\top} = S_{ct,ct}^{-1}$ and $S_{ct,t}^{\top} = S_{t,ct}$.

174 4.4. Generating solutions to the system

175 From the previous results, we can state the following.

Theorem 4. Given a vector \mathbf{b} satisfying (16), all solutions of (8) look like $\mathbf{a} = [\mathbf{a}_{ct}, \mathbf{a}_t]^{\top}$ with

$$\forall \mathbf{a}_t, \quad \mathbf{a}_{ct} = S_{ct,ct}^{-1} (\mathbf{b}_{ct} - S_{ct,t} \mathbf{a}_t). \quad (17)$$

Proof of Theorem 4. All vectors \mathbf{a} , with blocks defined in (17), verifies the first block line of system (13). To get the second block line of (13), let us multiply \mathbf{a}_{ct} in (17) by $S_{t,ct}$ and rearrange the terms, we thus obtain

$$S_{t,ct} \mathbf{a}_{ct} + S_{t,ct} S_{ct,ct}^{-1} S_{ct,t} \mathbf{a}_t = S_{t,ct} S_{ct,ct}^{-1} \mathbf{b}_{ct}. \quad (18)$$

Then using $S_{t,t} = S_{t,ct} S_{ct,ct}^{-1} S_{ct,t}$ and the condition (16) for \mathbf{b} , relation (18) becomes

$$S_{t,ct} \mathbf{a}_{ct} + S_{t,t} \mathbf{a}_t = \mathbf{b}_t, \quad (19)$$

that is the second line block of (13). The other way around, from the first line block of (13) we can set $\mathbf{a}_{ct} = S_{ct,ct}^{-1} (\mathbf{b}_{ct} - S_{ct,t} \mathbf{a}_t)$ since $S_{ct,ct}$ is invertible. We replace \mathbf{a}_{ct} in the second line block of (13) and we have

$$-S_{t,ct} S_{ct,ct}^{-1} S_{ct,t} \mathbf{a}_t + S_{t,t} \mathbf{a}_t = \mathbf{b}_t - S_{t,ct} S_{ct,ct}^{-1} \mathbf{b}_{bc}.$$

176 The right-hand-side \mathbf{b} verifies (16) thus $\mathbf{b}_t - S_{t,ct} S_{ct,ct}^{-1} \mathbf{b}_{bc} = \mathbf{0}$. Therefore we have
177 $S_{\Gamma} \mathbf{a}_t = \mathbf{0}$ with $S_{\Gamma} = 0$ thus \mathbf{a}_t can be any vector in \mathbb{R}^{d_L+p} . \square

To summarize, the infinite set of solutions to (8) with the form $[\mathbf{a}_{ct}, \mathbf{a}_t]$, is generated by *arbitrarily* setting the entries of the block \mathbf{a}_t and by computing \mathbf{a}_{ct} with the system

$$S_{ct,ct}\mathbf{a}_{ct} = \mathbf{b}_{ct} - S_{ct,t}\mathbf{a}_t. \quad (20)$$

178 The solution of system (8) is thereby reduced to the components indexed out of a
 179 tree, namely to \mathbf{a}_{ct} , once the block \mathbf{a}_t has been set. We say that we impose the classical *tree*
 180 *gauge* when we set $\mathbf{a}_t = \mathbf{0}$. It is worth noting that these tree gauges are not a discretization
 181 of the Coulomb gauge stated in (5) or (6). We follow this way in the next section.

182 5. The discrete Coulomb gauge

We have seen that the dof block \mathbf{a}_t of the magnetic vector potential \mathbf{A}_h is set arbitrarily, eventually equal to zero, without affecting the corresponding field $\mathbf{B}_h = \text{curl}\mathbf{A}_h$. We now start from condition (10), that is, we restrict the solution \mathbf{a} of $S\mathbf{a} = \mathbf{b}$ to verify $\mathbf{a} \in (\ker(S))^\perp = \text{Im}(S)$. We thus have to look for a vector $\mathbf{a} = T^\top \mathbf{y}$ where $T = \begin{bmatrix} S_{ct,ct} & S_{ct,t} \end{bmatrix}$ is the block ct of rows in S . In fact, according to Theorem 2, we have $\mathbf{a} \in \text{Im}(S)$ if and only if \mathbf{a} has the form

$$\begin{bmatrix} \mathbf{a}_{ct} \\ S_{t,ct} S_{ct,ct}^{-1} \mathbf{a}_{ct} \end{bmatrix} = \begin{bmatrix} I_{ct} \\ S_{t,ct} S_{ct,ct}^{-1} \end{bmatrix} \mathbf{a}_{ct} = \underbrace{\begin{bmatrix} S_{ct,ct} \\ S_{t,ct} \end{bmatrix}}_{T^\top} \underbrace{S_{ct,ct}^{-1} \mathbf{a}_{ct}}_{\mathbf{y}} = T^\top \mathbf{y},$$

183 with I_{ct} denoting the identity matrix for the block ct .

Applying the *discrete Coulomb gauge* means to look for a vector $\mathbf{y} \in \mathbb{R}^{[d_N - (d_L + p)]}$ such that $S T^\top \mathbf{y} = \mathbf{b}$. Using this change of variable $\mathbf{a} = T^\top \mathbf{y}$, from \mathbf{a} to \mathbf{y} , by relying on the block definition of T and S , the relation $S T^\top \mathbf{y} = \mathbf{b}$ can be written as

$$\begin{bmatrix} T \\ M \end{bmatrix} T^\top \mathbf{y} = \mathbf{b}, \quad M = \begin{bmatrix} S_{t,ct} & S_{t,t} \end{bmatrix}.$$

Hence, the discrete Coulomb gauge consists in looking for *the* solution of $S\mathbf{a} = \mathbf{b}$ of the form $\mathbf{a} = T^\top \mathbf{y}$ with \mathbf{y} solving the system

$$T T^\top \mathbf{y} = \mathbf{b}_{ct}. \quad (21)$$

184 The ones of T are the rows of S with indices in ct and hence they span all the rowspace
 185 of S , since $S_{ct,ct}$ is maximal rank, namely $\text{Row}(S) = \text{Row}(T)$. The matrix $T T^\top$ is square,
 186 symmetric and positive definite, since T is full rank. It can be inverted by efficient, direct
 187 or iterative, techniques well-known in scientific computing.

188 Under the compatibility conditions on \mathbf{b} stated in Theorem 2, the lower part
 189 $M T^\top \mathbf{y} = \mathbf{b}_t$ of the system $S T^\top \mathbf{y} = \mathbf{b}$ is redundant with the upper one given in
 190 (21). Let us perform the matrix products:

191 (i) $T T^\top \mathbf{y} = \mathbf{b}_{ct}$ that is $(S_{ct,ct} S_{ct,ct} + S_{ct,t} S_{t,ct}) \mathbf{y} = \mathbf{b}_{ct}$.

192 (ii) $M T^\top \mathbf{y} = \mathbf{b}_t$ that is $(S_{t,ct} S_{ct,ct} + S_{t,t} S_{t,ct}) \mathbf{y} = \mathbf{b}_t$.

If \mathbf{b} verifies (16), from (i) we get (ii). Indeed

$$\begin{aligned} (S_{ct,ct} S_{ct,ct} + S_{ct,t} S_{t,ct}) \mathbf{y} &= \mathbf{b}_{ct}, \\ (S_{ct,ct} + S_{ct,ct}^{-1} S_{ct,t} S_{t,ct}) \mathbf{y} &= S_{ct,ct}^{-1} \mathbf{b}_{ct}, \\ (S_{t,ct} S_{ct,ct} + \underbrace{S_{t,ct} S_{ct,ct}^{-1} S_{ct,t}}_{S_{t,t}} S_{t,ct}) \mathbf{y} &= \underbrace{S_{t,ct} S_{ct,ct}^{-1} \mathbf{b}_{ct}}_{\mathbf{b}_t} \\ MT^\top \mathbf{y} &= \mathbf{b}_t. \end{aligned}$$

193 We can fix some expressions. The original problem is to solve $S\mathbf{a} = \mathbf{b}$ under the com-
 194 patibility condition on \mathbf{b} . The tree allows to find $S_{ct,ct}$ invertible, thus to prepare S in

195 a block form. To impose a *discrete Coulomb gauge* on (13) means to select solutions of
 196 such a problem of the form $\mathbf{a} = T^\top \mathbf{y}$. To solve (13) under the discrete Coulomb gauge is
 197 equivalent to solve the *gauged problem* $ST^\top \mathbf{y} = \mathbf{b}$, in particular $TT^\top \mathbf{y} = \mathbf{b}_{ct}$ since the
 198 rest of the equations (those with right-hand-side \mathbf{b}_i) are redundant.

199
 200 **Remark:** Note that the null space gauge was enforced by the change of variable from
 201 \mathbf{a} to \mathbf{y} , that actually enforces the orthogonality of \mathbf{a} to the kernel of S (that is the same
 202 as the kernel of R). We have indicated previously that the kernel of R include all the
 203 gradients. In this sense, with the imposition of the discrete Coulomb gauge, we have
 204 computed a magnetic vector potential \mathbf{A}_h that is orthogonal to all gradients of nodal
 205 functions in W_*^0 , namely, that fulfills (6).

206 6. Other formulations in magnetostatics

207 Alternative formulations, with respect to the magnetic vector potential one, exploit
 208 the zero divergence condition of the source \mathbf{J} . The starting point is the magnetostatic
 209 problem in terms of the magnetic field \mathbf{H} . Namely, assigned a solenoidal source current
 210 \mathbf{J} with $\text{supp}(\mathbf{J}) \subset \Omega$, we wish to compute the magnetic field \mathbf{H} defined in Ω from the
 211 equations $\text{curl } \mathbf{H} = \mathbf{J}$, $\text{div}(\mu \mathbf{H}) = 0$, with boundary conditions $\mu \mathbf{H} \cdot \mathbf{n}_{\partial\Omega} = 0$ and
 212 $\int_{\Omega} \mathbf{H} \cdot \mathbf{v} = 0$ for all $\mathbf{v} \in \mathcal{H}_\mu(m; \Omega)$. As commonly done [1,12,13], the condition $\text{div } \mathbf{J} = 0$
 213 is strongly satisfied via a curl-conforming source field, namely an electric vector potential
 214 \mathbf{T} such that $\mathbf{J} = \text{curl } \mathbf{T}$. Again, the problem $\text{curl } \mathbf{T} = \mathbf{J}$ is overdetermined, since the
 215 kernel of the curl operator includes the gradients. If Ω is not simply connected, there
 216 exist vector fields in $H^0(\text{curl}; \Omega) = \{\mathbf{w} \in H(\text{curl}; \Omega), \text{curl } \mathbf{w} = \mathbf{0}\}$ that are not gradients.
 217 Indeed, the dimension of the quotient space $H^0(\text{curl}; \Omega) / \text{grad}(H^1(\Omega))$ coincides with
 218 $b_1(\Omega)$. We can thus apply analogous gauging techniques as the ones we have analysed
 219 before to solve it. In this case, a *belted tree* is used (see, e.g., [14]).

220 We have seen that a spanning tree on the graph of the gradient operator is involved
 221 in both the discrete version resolution of (1) and (2). There is however a difference
 222 between the construction of a spanning tree, say \mathcal{T}_b^G , when working in terms of \mathbf{B} and
 223 that of say \mathcal{T}_a^G when working in terms of \mathbf{A} . We have indeed that \mathcal{T}_b^G can be a belted
 224 tree, that takes into account $b_1(\Omega)$, the first Betti number of Ω (e.g., [14]) whereas \mathcal{T}_a^G is a
 225 genuine spanning tree of a graph that pays attention to $b_2(\Omega)$, the second Betti number
 226 of Ω . This is much related to the type of boundary conditions appearing in (1) and (2).
 227 The condition on $\mathbf{A} \times \mathbf{n}_{\partial\Omega}$ takes in the $p + 1$ connected components of $\partial\Omega$. Here we
 228 work in terms of \mathbf{A} , so \mathcal{T}^G is of type \mathcal{T}_a^G . Similar considerations can be stated for the
 229 graph to consider when we have to build a tree for the solution of the magnetostatic
 230 problem in either \mathbf{H} or \mathbf{T} .

231 7. Discussion and concluding remarks

232 Using, as dofs for the first family of Nédélec FEs, the weights, it is natural to
 233 extend the classical tree-cotree techniques to high-order approximations. The idea in this
 234 work is to recall the main problems where this type of techniques are applied. We pay
 235 particular attention to the generality of the domain from a topological point of view and
 236 the implication that this generality has on the graph (and consequently on the spanning
 237 tree) to be considered. We have considered in detail the use of the tree-cotree technique
 238 when looking for a solution of the magnetostatic problem in terms of a magnetic vector
 239 potential \mathbf{A} in a general domain Ω . We have deeply analysed, in the high order FE
 240 context, the two different ways of performing a discrete gauge that were considered
 241 by Manges and Cendes in the low order case. We have recalled also briefly the use of
 242 this technique for the computation of an electric vector potential \mathbf{T} when solving the
 243 magnetostatic problem in terms of the magnetic field \mathbf{H} .

244 In these pages, we have proved some properties for the linear system with matrix
 245 S associated with a high order edge FE discretization of the magnetostatic problem in
 246 terms of the magnetic vector potential \mathbf{A} . By relying on a tree-cotree partition of the

247 components of the solution vector \mathbf{a} , Theorem 2 states that $\mathbf{a} \in \ker(S)$ if and only if
 248 $\mathbf{a}_{ct} = -S_{ct,ct}^{-1} S_{ct,t} \mathbf{a}_t$. Then, to have $\mathbf{a} \in (\ker(S))^\perp$, when imposing the discrete Coulomb
 249 gauge, we look for a solution of the form $\mathbf{a} = T^\top \mathbf{y}$. Under the compatibility condition on
 250 the right-hand-side of Theorem 2, both the tree and discrete Coulomb gauges allow to
 251 construct a solution of $S \mathbf{a} = \mathbf{b}$. The tree-cotree technique in Theorem 1 allows to define
 252 the block of maximal rank in S and thus to define T . The tree gauge chooses the solution
 253 \mathbf{a} by fixing the entries of the block $\mathbf{a}_t = \mathbf{0}$, in agreement with (17). However, these entries
 254 collected in \mathbf{a}_t can be arbitrarily fixed and when they are different from zero, we have
 255 another gauge.

256 **Funding:** This research was funded by the French National Research Agency grant MathIT number
 257 ANR-15-IDEX-01 and the Italian project PRIN 201752HKH8.

References

1. Albanese, R.; Rubinacci, G. Magnetostatic field computations in terms of two-component vector potentials. *Int. J. Numer. Meth. Engng.* **1990**, *29*, 515–532.
2. Manges, J.B.; Cendes, Z.J. A generalized tree-cotree gauge for magnetic field computation. *IEEE Transactions on Magnetics* **1995**, *31*, 1342–1347.
3. Bossavit, A. Whitney forms: A class of finite elements for three-dimensional computations in electromagnetism. *IEE Proceedings A (Physical Science, Measurement and Instrumentation, Management and Education, Reviews)* **1988**, *135*, 493–500.
4. Rapetti, F.; Bossavit, A. Whitney forms of higher degree. *SIAM J. Numer. Anal.* **2009**, *47*, 2369–2386. doi:10.1137/070705489.
5. Whitney, H. *Geometric integration theory*; Princeton University Press: Princeton, N. J., 1957.
6. Alonso Rodríguez, A.; Valli, A. *Eddy Current Approximation of Maxwell Equations*; Vol. 4, *Modeling, Simulation & Applications*, Springer-Verlag, Italia, 2010.
7. Arnold, D.N.; Falk, R.S.; Winther, R. Finite element exterior calculus, homological techniques, and applications. *Acta Numer.* **2006**, *15*, 1–155. doi:10.1017/S0962492906210018.
8. Christiansen, S.; Rapetti, F. On high order finite element spaces of differential forms. *Mathematics of Computation* **2016**, *85*, 517–548.
9. Alonso Rodríguez, A.; Bruni Bruno, L.; Rapetti, F. Minimal sets of unisolvent weights for high order Whitney forms on simplices. In *Numerical mathematics and advanced applications—Enumath 2019*; Lect. Notes Comput. Sci. Eng., Springer, Cham, 2020; pp. 195–203.
10. Rapetti, F.; Alonso Rodríguez, A. High Order Whitney Forms on Simplices and the Question of Potentials. In *Numerical mathematics and advanced applications—Enumath 2019*; Lect. Notes Comput. Sci. Eng., Springer, Cham, 2020; pp. 1–16.
11. Quarteroni, A.; Valli, A. *Numerical approximation of partial differential equations*; Vol. 23, *Springer Series in Computational Mathematics*, Springer-Verlag, Berlin, 1994; pp. xvi+543.
12. Carpenter, C. Comparison of alternative formulations of 3-dimensional magnetic-field and eddy-current problems at power frequencies. Proceedings of the Institution of Electrical Engineers. IET, 1977, Vol. 124, pp. 1026–1034.
13. Dular, P.; Peng, P.; Geuzaine, C.; Sadowski, N.; Bastos, J. Dual magnetodynamic formulations and their source fields associated with massive and stranded inductors. *IEEE Transactions on Magnetics* **2000**, *36*, 1293–1299.
14. Rapetti, F.; Dubois, F.; Bossavit, A. Discrete vector potentials for nonsimply connected three-dimensional domains. *SIAM J. Numer. Anal.* **2003**, *41*, 1505–1527.